Eur. Phys. J. B **35**, 223–232 (2003)
DOI: 10.1140/epjb/e2003-00272-6

THE EUROPEAN PHYSICAL JOURNAL B

Dynamical CPA approach to an itinerant fermionic spin glass model

M. Bechmann[a] and R. Oppermann

Institut für Theoretische Physik und Astrophysik, Universität Würzburg, 97074 Würzburg, Federal Republic of Germany

Received 29 June 2003 / Received in final form 5 August 2003
Published online 2 October 2003 –

Abstract. We study a fermionic version of the Sherrington-Kirkpatrick model including nearest-neighbor hopping on a ∞-dimensional simple cubic lattices. The problem is reduced to one of free fermions moving in a dynamical effective random medium. By means of a CPA method we derive a set of self-consistency equations for the spin glass order parameter and for the Fourier components of the local spin susceptibility. In order to solve these equations numerically we employ an approximation scheme which restricts the dynamics to a feasible number of the leading Fourier components. From a sequence of systematically improved dynamical approximations we estimate the location of the quantum critical point.

PACS. 75.10.Nr Spin glass and other random models – 75.40.Cx Dynamic properties – 71.10.Fd Lattice fermion models

1 Introduction

Quantum-dynamical mean field theories are highly appreciated, helpful methods to provide insight into models of strongly interacting systems [1]. A well-known case is certainly the Hubbard model including its various model ramifications. Fermionic spin glass models, though describing the quite different physics of randomly interacting disordered systems, belong to this category as well; in particular, they also deal with an intense interplay between magnetism and transport properties.

Quantum dynamics in systems with random many-body interactions are known to contain a challenging technical difficulty which arises from the double-time dependence of the spin glass field. This feature of quantum spin dynamics is hard to handle even in the dynamical mean field theory (DMFT) and requires further simplifications, such as the limit $M \to \infty$ in $SU(M)$-generalizations of spin systems [2].

In earlier work the so-called static approximation (defined by a static effective spin glass field) was used to construct a systematic low temperature expansion for metallic spin glasses [3]. The quantum critical point was determined within this approximation. Later, a Ginzburg-Landau theory [4], which kept only terms relevant or dangerously irrelevant under the quantum dynamical renormalization group, was applied to study the critical exponents.

Within this framework it turned out that the quantum-dynamical Gaussian result for the shift exponent of the critical temperature disagreed with the static approximation result due to the effect of dangerously irrelevant dynamic couplings. The shift exponent ϕ can be defined by $T_c(x) \sim (x_c - x)^\phi$, $x_c > x$, where x stands for the parameter which drives the quantum phase transition, and $T_c(x_c)$ vanishes by definition at the quantum critical point (QCP).

Naturally, renormalization groups are not designed to determine critical points. However, the positions of the QCPs are relevant, too. In finite dimensions the magnetic transition may coincide with a localization transition driven by the randomness of the many-body interaction. If these transitions do not coincide it is still important to know whether or not the magnetic transition occurs within the metallic phase and, perhaps, to identify parameters which influence the relative position of the QCPs. The answer may in some detail be model-dependent, but a coincidence of both transitions would almost certainly contain deeper reasons and could be expected to appear at least in model classes.

In this work we adapt and apply the coherent potential approximation (CPA) to a metallic spin glass problem. Originally this powerful non-perturbative method was developed to describe non-interacting disordered electron systems [5], and in this context the CPA can be shown to become exact in the limit of infinite spatial dimensions ($d \to \infty$) [6]. Later, the CPA formalism was generalized to deal with interacting electron systems [7,8] with

[a] e-mail: bechmann@physik.uni-wuerzburg.de

highly non-trivial couplings of the Matsubara frequencies. Finally, the CPA method can also be applied to dynamical disorder. Like in the present work, this situation for instance results from the dynamical decoupling of interaction terms [9].

It is interesting to note that effective action terms that are non-diagonal in imaginary time not only occur in the presence of disorder. For certain translationally invariant models, the so-called extended DMFT approach [10], which to some extend incorporates spatial correlations, gives rise to effective impurity problems equivalent to the one studied in this article.

The present article is organized as follows. The required technical tools and strategies are developed in Section 2. After the model definition we give a brief description of the dynamical two-step decoupling procedure, which reduces the problem to one of free fermions moving in a dynamical random magnetic field. The model assumption of a fully connected magnetic interaction facilitates a saddle point treatment. Extending previous work [3,11] we choose a *dynamical* self-consistent saddle point for the spin glass field.

The quantum-dynamical CPA method, shaped to apply to the present quantum spin glass model, is discussed in Section 2.2. Within this framework, a set of replica-symmetric self-consistency equations for the saddle point values q (spin glass order parameter) and $\tilde{q}_m = \tilde{q}(\omega_m)$ (the local replica diagonal spin correlation) are derived. As the centerpiece we obtain a matrix CPA-equation in Matsubara frequency space.

Our ideas for the approximate solution of these self-consistency equations are introduced in Section 2.3. As a systematic approximation scheme we propose to restrict the dynamics of the effective random medium to a number of bosonic Matsubara frequencies that can be numerically dealt with. Similar approximations have been constructed earlier in the context of the Ising spin glass in the transverse field by means of discretization of the imaginary time axis [12,13].

Section 3 revisits the spin-static approximation where a crucial simplification arises: the matrix structure of the equations disappears. In particular, the CPA-equation can be solved independently for each Matsubara frequency. However, *via* the saddle point values, the non-trivial coupling of the frequencies is preserved also in the static set of self-consistency equations. We present numerical solutions for all temperatures including $T = 0$. The spin-static $T = 0$ critical point well agrees with the results for an earlier model version [3].

The main results follow in Section 4. We evaluate the critical line in the T–t plane (t represents the hopping strength) as a sequence of improved dynamical approximations, which helps to derive the decay of the critical temperature towards the quantum critical point. This dynamical approximation scheme is not designed to capture the zero-temperature limit. But, by increasing the number of Fourier components of the effective random medium, one finds the T_c-deviation from the spin-static approximation result almost accurately down to lower and lower temperatures. It is seen that the higher-frequency corrections to T_c are small; their infinite number accumulates and leads to the non-analytical behavior of the T_c-curve for $T_c \to 0$. From the characteristic decay of these corrections we deduce the location of the QCP. The numerical results also fit with the quantum-dynamical shift exponent of the T_c-curve and thus provide a reliable estimate of the QCP's position.

2 Effective action and construction of the self-consistency method

2.1 Model and spin glass decoupling procedure

We consider the grand canonical Hamiltonian

$$\mathcal{K} = \frac{1}{2}\sum_{i\neq j} J_{ij} S_i^z S_j^z \; - \; \mu \sum_{i\sigma} a_{i\sigma}^\dagger a_{i\sigma} \; + \; \tilde{t} \sum_{\langle ij\rangle \sigma} a_{i\sigma}^\dagger a_{j\sigma} \quad (1)$$

with the fermionic Ising spin operators given by $S_i^z = a_{i\uparrow}^\dagger a_{i\uparrow} - a_{i\downarrow}^\dagger a_{i\downarrow}$. The sum index $\langle ij\rangle$ in the hopping term denotes summation over nearest-neighbor lattice sites. We assume quenched Gaussian disorder among the magnetic coupling constants J_{ij} according to the distribution

$$P(J_{ij}) = \frac{1}{\sqrt{2\pi}\tilde{J}} \exp\left(-\frac{J_{ij}^2}{2\tilde{J}^2}\right). \quad (2)$$

In distinction to previous work [3,11,14] there is no disorder in the kinetic part of (1). In order to facilitate the solution of this model we assume a fully connected magnetic interaction among the N lattice sites. The hopping takes place on an underlying simple cubic lattice in the limit of infinite spatial dimensions d. To obtain physically meaningful results we apply the usual scaling of the model parameters [15]

$$\tilde{J} = J/\sqrt{N} \quad \text{and} \quad \tilde{t} = t/\sqrt{d}. \quad (3)$$

To some extent the derivation of the self-consistency equations of the present model follows the detailed discussion given in [11]. In the following we restrict ourselves to a brief outline of the two-step decoupling procedure in the replica formalism.

We start from the Grassmann field theoretic formulation of the n-fold replicated partition function. The disorder average, *i.e.* integration over the magnetic coupling constants with the Gaussian weight (2) generates four-spin products in the effective action. Due to the assumed complete connectivity of the magnetic interaction these four-spin products can be reduced to quadratic terms by means of site-global, replica and imaginary-time dependent real decoupling fields $Q_{\alpha\beta}^{\tau\tau'}$. The disorder averaged replicated partition function at this stage reads

$$[Z^n]_J = c^n \int \mathcal{D}\, Q \int \mathcal{D}\, \Psi \, \mathrm{e}^{-\mathcal{A}_0 - \mathcal{A}_t - \mathcal{A}_J} \quad (4)$$

with the action terms

$$\mathcal{A}_0 = \sum_{i\alpha\sigma} \int_\tau \bar{\Psi}^\tau_{i\alpha\sigma} \left(\partial_\tau - \mu\right) \Psi^\tau_{i\alpha\sigma}, \tag{5}$$

$$\mathcal{A}_t = \tilde{t} \sum_{\substack{(ij)\\ \alpha\sigma}} \int_\tau \bar{\Psi}^\tau_{i\alpha\sigma} \Psi^\tau_{j\alpha\sigma}, \tag{6}$$

$$\mathcal{A}_J = \frac{J^2}{4} \int_{\tau\tau'} \sum_{\substack{\alpha,\beta\\ i}} \left(\left(Q^{\tau\tau'}_{\alpha\beta}\right)^2 - 2 Q^{\tau\tau'}_{\alpha\beta}\, \mathcal{S}^\tau_{i\alpha} \mathcal{S}^{\tau'}_{i\beta} \right). \tag{7}$$

Here $\mathcal{S}^\tau_{i\alpha} = \sum_\sigma \bar{\Psi}^\tau_{i\alpha\sigma} \sigma \Psi^\tau_{i\alpha\sigma}$ is the time dependent Grassmann representation of an Ising spin operator and the τ-integrations extend from 0 to the inverse temperature $1/T$.

The further evaluation of (4) relies on the elimination of the fields $Q^{\tau\tau'}_{\alpha\beta}$ by means of a saddle point integration. The simplest but by no means trivial way to proceed would be the assumption of a replica-symmetric and static (*i.e.* $\tau\tau'$-independent) saddle point [3,11]. Since we want to explore however the role played by the quantum dynamics, we have to keep the time dependence.

Let us symbolize the quantum statistical average and the disorder average by $\langle\,\rangle$ and $[\,]_J$, respectively. Then, the saddle point matrix can be expressed in terms of the corresponding averaged spin products:

$$Q^{\tau\tau'}_{\alpha\neq\beta}\Big|_{\text{s.p.}} = \left[\left\langle \mathcal{S}^\tau_{i\alpha} \mathcal{S}^{\tau'}_{i\beta} \right\rangle^{\alpha\neq\beta} \right]_J = \left[\langle \mathcal{S}^0_{i\alpha} \rangle \langle \mathcal{S}^0_{i\beta} \rangle \right]_J \tag{8}$$

$$Q^{\tau\tau'}_{\alpha\alpha}\Big|_{\text{s.p.}} = \left[\left\langle \mathcal{S}^\tau_{i\alpha} \mathcal{S}^{\tau'}_{i\alpha} \right\rangle \right]_J = \left[\left\langle \mathcal{S}^{\tau-\tau'}_{i\alpha} \mathcal{S}^0_{i\alpha} \right\rangle \right]_J. \tag{9}$$

Clearly, the inter-replica spin correlations are independent of time because the fermions can not propagate between different replications of the system. All quantum-dynamical behavior of the model originates from the diagonal elements of the saddle point matrix.

In this publication we choose a global replica-symmetric saddle point (which is approximate only below T_c, but does not affect the T_c-result of the second order phase transition) with the appropriate time dependence according to (8, 9),

$$Q^{\tau\tau'}_{\alpha\neq\beta}\Big|_{\text{s.p.}} = q \quad \text{and} \quad Q^{\tau\tau'}_{\alpha\alpha}\Big|_{\text{s.p.}} = \tilde{q}_{|\tau-\tau'|}. \tag{10}$$

We prefer to work in frequency space and perform Fourier transformations of the Grassmann variables as well as of the diagonal part of the saddle point matrix which take the form

$$\Psi^\tau = T \sum_{l=-\infty}^{\infty} \Psi^l \, \mathrm{e}^{-i z_l \tau}, \tag{11}$$

$$\tilde{q}_{|\tau-\tau'|} = \sum_{m=-\infty}^{\infty} \tilde{q}_m \, \mathrm{e}^{-i\omega_m(\tau-\tau')}, \tag{12}$$

where z_l and ω_m denote fermionic and bosonic Matsubara frequencies, respectively. The Fourier coefficients $\tilde{q}_m$ are real quantities and obey the symmetry relation $\tilde{q}_m = \tilde{q}_{-m} = \tilde{q}^*_m$.

In order to facilitate the Grassmann integration the effective action must be further reduced to a quadratic form of the Grassmann variables which requires another decoupling step. Without going into detail we hence introduce Gaussian integrations over site-local and replica-global fields z_i and site-local and replica-global fields $y_{i\alpha}$. The latter again split into $y_{i\alpha 0}$, which are also present in the spin-static theory, and dynamical decoupling fields $y^\pm_{i\alpha m\geq 1}$, which comprise the quantum dynamical character of the model.

Introduction of a space saving definition. Throughout this article we will use the shorthand notation of the Gaussian integral operator

$$\int_x^G f(x) = \frac{1}{\sqrt{2\pi}} \int_{-\infty}^{\infty} \mathrm{d}x \, \exp\left(-\frac{x^2}{2}\right) f(x) \tag{13}$$

which renders many of the equations more compact.

Employing this abbreviation we arrive at the completely decoupled partition function

$$[Z^n]_J = c^n \prod_i \int_{z_i}^G \prod_{i\alpha} \int_{y_{i\alpha 0}}^G \prod_{\substack{i\alpha\\ m\geq 1}} \int_{y^+_{i\alpha m}}^G \int_{y^-_{i\alpha m}}^G \int \mathcal{D}\Psi \, \mathrm{e}^{-\mathcal{A}_{\text{eff}}} \tag{14}$$

with the effective action

$$\begin{aligned} \mathcal{A}_{\text{eff}} =& \frac{nNJ^2}{4T^2} \left(\sum_m \tilde{q}^2_m - q^2 \right) + \mathcal{A}_t \\ & - T \sum_{i\alpha\sigma l} \left(i z_l + \mu + \sigma H^0_{i\alpha} \right) \bar{\Psi}^l_{i\alpha\sigma} \Psi^l_{i\alpha\sigma} \\ & - T \sum_{\substack{i\alpha\sigma l\\ m\geq 1}} \sigma \left(H^m_{i\alpha} \bar{\Psi}^{l+m}_{i\alpha\sigma} \Psi^l_{i\alpha\sigma} \, + \, H^{m*}_{i\alpha} \bar{\Psi}^{l-m}_{i\alpha\sigma} \Psi^l_{i\alpha\sigma} \right). \end{aligned} \tag{15}$$

In equation (15) we discarded irrelevant terms $\sim n^2$. The occurring effective magnetic fields, which are complex, dynamical, and local in site- and replica-indices, are given by

$$H^0_{i\alpha} = J \left(\sqrt{q}\, z_i \, + \, \sqrt{\tilde{q}_0 - q}\, y_{i\alpha 0} \right), \tag{16}$$

$$H^{m\geq 1}_{i\alpha} = J \sqrt{\frac{\tilde{q}_m}{2}} \left(y^+_{i\alpha m} + i y^-_{i\alpha m} \right). \tag{17}$$

2.2 The dynamical CPA approach

According to equations (14, 15) the problem has been reduced to an ensemble of non-interacting fermions moving in a complex replica- and spin-dependent effective random medium. This situation immediately calls for a dynamical version of the CPA [9]. Following the prescription of this method we replace the complex random medium $H^m_{i\alpha}$ by a yet unknown self energy Σ_l. The chosen limit of infinite spatial dimensions simplifies the problem to a single site

problem and justifies the assumption of a site-diagonal (or k-independent) self-energy [1,6].

The effective action (15) is not diagonal in the energy indices thus allowing for virtual absorption and emission of dynamical field quanta $H_{i\alpha}^{m\geq 1}$. However, the full fermion Green's function of the original interacting problem with any realization of the quenched disorder is certainly energy conserving and so is the full disorder averaged Green's function. Hence its off-diagonal elements in frequency space must vanish due to the average over the effective random medium. There is also no ferromagnetic tendency in the system which altogether justifies our ansatz of a spin-independent and frequency-diagonal self-energy.

In order to determine Σ_l self-consistently we keep the random medium at one single site, say $i = 0$. The effective action then reads

$$\mathcal{A}_{\text{eff}}^{CPA} = \frac{nNJ^2}{T^2}\sum_m \left(\tilde{q}_m^2 - q^2\right) - T\sum_{\substack{ij\\ \alpha\sigma l' l}} \bar{\Psi}_{i\alpha\sigma}^l \left(\left(\mathsf{G}^{-1}\right)_{ij}^{l'l} - V_{\alpha\sigma}^{l'l}\delta_{i0}\delta_{j0}\right)\Psi_{j\alpha\sigma}^l \quad (18)$$

with the inverse of the full disorder averaged Green's function

$$\left(\mathsf{G}^{-1}\right)_{ij}^{l'l} = \left(\left(iz_l + \mu - \Sigma_l\right)\delta_{ij} + \tilde{t}\,\delta_{\langle ij\rangle}\right)\delta_{l'l} \quad (19)$$

and the effective dynamical potential at the special lattice site $i = 0$

$$V_{\alpha\sigma}^{l'l} = \begin{cases} \sigma H_{0\alpha}^m, & l' = l + m, m > 0 \\ \sigma H_{0\alpha}^0 + \Sigma_l, & l' = l \\ \sigma H_{0\alpha}^{m\,*}, & l' = l - m, m > 0. \end{cases} \quad (20)$$

In the assumed case of infinite spatial dimensions nearest-neighbor hopping of non-interacting particles is described by the function (recall the scaling (3))

$$T_0(x,t) = -\text{sign}(\text{Im}\,x)\frac{\sqrt{\pi}}{2t}\exp\left(-\frac{x^2}{4t^2}\right)\left(i + \text{erfi}\frac{x}{2t}\right) \quad (21)$$

which reveals for $x = \varepsilon + i0^+$ the well-known Gaussian density of states [15,16]. Hence the full Green's function G defined in (19) is readily expressed by

$$(\mathsf{G})_{ij} = \mathsf{T}\delta_{ij} + \mathcal{O}\left(\frac{1}{\sqrt{d}}\right) \quad (22)$$

where T is site independent and diagonal in the Matsubara indices:

$$(\mathsf{T})_{l'l} = T_0\left(iz_l + \mu - \Sigma_l, t\right)\delta_{l'l}. \quad (23)$$

For the formulation of the self-consistency equations it is useful to define as an auxiliary quantity the site-local propagator at site $i = 0$ in the presence of the effective potential,

$$(\Gamma_{\alpha\sigma})_{l'l} = T\left\langle \bar{\Psi}_{0\alpha\sigma}^l \Psi_{0\alpha\sigma}^{l'}\right\rangle_{\mathcal{A}_{\text{eff}}^{\text{CPA}}} = \left(\left[\mathsf{T}^{-1} + \mathsf{V}_{\alpha\sigma}\right]^{-1}\right)_{l'l}. \quad (24)$$

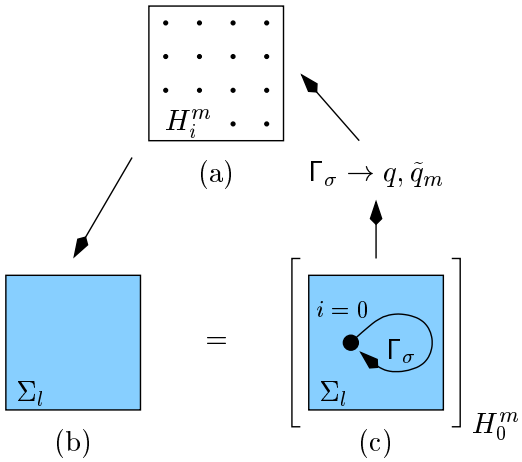

Fig. 1. Structure of the self-consistency problem of the itinerant spin glass model (inspired by [8]). (a) indicates the effective dynamical random medium H_i^m, which depends on the spin glass order parameter q and the replica-diagonal saddle point $\tilde{q}_m$ (Eqs. (16, 17)). (b) and (c) illustrate the determination of the homogeneous self-energy Σ_l by the CPA-equation (25). From the local propagator Γ_σ at the special lattice site $i = 0$ the physical quantities q and $\tilde{q}_m$ are constructed, which in turn generate the original random medium in (a).

In essence, within the CPA method the frequency-dependent self-energy Σ_l is determined by the demand that the average of the local propagator matrix $\Gamma_{\alpha\sigma}$ at the special site $i = 0$ with respect to the dynamical potential (20) coincides with the local part of the full disorder averaged homogeneous Green's function, T (see Fig. 1). Note that equating both quantities requires the replica limit $\lim_{n\to 0}$ to be taken.

Omitting the algebraic details we obtain the conditional matrix equation (to condense the notation all superfluous site-, replica-, or spin-indices are dropped from now on)

$$\mathsf{T} = \int_z^G [\Gamma_\sigma]_{\mathbf{y}}^{(z)} \quad (25)$$

where the symbol $[]_{\mathbf{y}}^{(z)}$ is a shorthand notation for the average with respect to all replica-local decoupling fields $\mathbf{y} = \{y_0, y_m^+, y_m^-\}$,

$$[f(z,\mathbf{y})]_{\mathbf{y}}^{(z)} = \frac{\int_{y_0}^G \prod_{m\geq 1}\int_{y_m^+}^G \int_{y_m^-}^G W(z,\mathbf{y}) f(z,\mathbf{y})}{\int_{y_0}^G \prod_{m\geq 1}\int_{y_m^+}^G \int_{y_m^-}^G W(z,\mathbf{y})}. \quad (26)$$

The weight function $W(z,\mathbf{y})$ that appears in (26) results from the integration of the Grassmann fields and is given by ($\text{Tr}_{l\sigma}$ comprises spin and frequency summation)

$$W(z,\mathbf{y}) = \exp\left(\text{Tr}_{l\sigma}\ln\left[1 + \mathsf{V}_\sigma\mathsf{T}\right]\right). \quad (27)$$

Note that, as discussed above, the off-diagonal elements of Γ_σ as well as its spin dependence vanish exactly by integration.

Expressions for the saddle point values (10) can be obtained by construction of the spin products given by

equations (8, 9) in terms of the Grassmann fields at the special lattice site $i = 0$ and application of Wick's theorem. After performing the Fourier transformation (11) and taking the replica limit $\lim_{n\to 0}$ the set of self-consistency equations is thus completed by

$$q = T^2 \int_z^G \left([\mathrm{Tr}_{l\sigma} \sigma \mathsf{\Gamma}_\sigma]_{\mathbf{y}}^{(z)} \right)^2 \tag{28}$$

$$\tilde{q}_m = T^2 \int_z^G \sum_{\substack{ll' \\ \sigma\sigma'}} \sigma\sigma' \times \left[\Gamma_\sigma^{l+m,l} \Gamma_{\sigma'}^{l'-m,l'} - \Gamma_\sigma^{l+m,l'+m} \Gamma_{\sigma'}^{l',l} \delta_{\sigma\sigma'} \right]_{\mathbf{y}}^{(z)} . \tag{29}$$

In (29) the first term involves the product of sums over the mth super- and sub-diagonals and the second the trace of the matrix product of two factors $\mathsf{\Gamma}_\sigma$ shifted against each other about m elements along the diagonal.

Note that in the limiting case of a vanishing hopping strength ($t \to 0$) equations (28, 29) correctly recover the results of the non-itinerant model [11] and with the additional choice of $\mu = -i\pi T/2$ [17] the equations further reduce to the SK-solution of the classical model [18].

2.3 General solution strategies

Any attempt to solve the set of self-consistency equations (25, 28, 29) faces the fundamental problem of the infinitely many quantities $\tilde{q}_m$ each of which effectuates corresponding Gaussian integrations *via* equations (16, 17, 27). In order to render the problem feasible we propose to keep only a few Fourier components $\tilde{q}_m$ with $m = \{0, \ldots, M\}$ and take the higher-frequency components to be zero, *i.e.* $\tilde{q}_{m>M} \equiv 0$. In turn this means that the Gaussian integrations associated with the components $\tilde{q}_{m>M}$ become trivial. Below we will refer to this approximation scheme as the "dynamical approximation of order M".

Within this approximation scheme the quantum dynamics is treated on energy scales ranging from $\omega_0 = 0$ to $\omega_M = 2\pi T M$. To estimate the quality of this approximation one has to compare the energy scales that are neglected to the hopping strength t as the model parameter that generates the quantum dynamics. Thus we are led to

$$t \ll \omega_{M+1} \equiv 2\pi T(M+1) \tag{30}$$

as a simple criterion of validity of the Mth order dynamical approximation. Hence, although it is neither a high temperature expansion nor an expansion in small t, the method works well especially for small t/T. In those regions in parameter space the approximation already at manageable low orders M excellently captures the effects of the quantum dynamics

Another difficulty arises from the infinite extension of the matrices T, V (which becomes a band matrix with M sub- and super-diagonals (20) in the dynamical approximation of order M) and $\mathsf{\Gamma}$ in frequency space. Naturally, a numerical analysis requires the restriction to finite matrices of size $2(l_c+1) \times 2(l_c+1)$, *i.e.* the matrices are constructed in the limited frequency range z_{-l_c-1} to z_{l_c}. However, there are also important contributions from higher frequencies that can not be neglected for accurate solutions.

We overcome this problem by systematic asymptotic expansions of the self-consistency equations in terms of $1/z_l$ up to some feasible order $\mathcal{O}\left((1/z_l)^K\right)$. Here we exploit the high-frequency asymptotics of the self-energy

$$\Sigma_l \underset{|l|\to\infty}{\longrightarrow} \sum_{k=1}^{K} a_k \left(i z_l\right)^{-(2k-1)} + \mathcal{O}\left(z_l^{-(2K+1)}\right) \tag{31}$$

where the expansion coefficients a_k are easy to calculate averages of polynomials of the effective fields (16, 17). The sums over the Matsubara frequencies which occur in equations (27, 28, 29) can always be split up into a low-frequency main part and a high-frequency part which are separated by the cut-off index l_c. While the matrix-structured main part has to be treated numerically the high-frequency contributions can be formulated in terms of asymptotic series expansions of docile structure that permits analytical summation.

The approximation of the high-frequency contributions by asymptotic series expansions introduces some error. The cut-off index l_c has to be chosen such that this error undershoots some given threshold of insignificance. In practical calculations we used different methods to determine l_c. A simple way is to make trial variations of the matrix size at each iteration cycle and to adjust (increase or decrease) l_c according to the corresponding variations of all relevant intermediate quantities. A more direct method is to evaluate the contributions of the first neglected asymptotic order, *i.e.* $\mathcal{O}\left((1/z_l)^{K+1}\right)$, as a function of l_c and to apply some suitable smallness criterion. The latter method turned out to be un-practical for $M > 0$ because of the complexity of the occurring analytical expressions for the asymptotic Matsubara sums.

The final criterion for l_c is always that the physical quantities are independent of this auxiliary parameter at some desired level of precision. The proper choice of l_c and thereupon the computational expenses for solving the self-consistency equations strongly depend on the temperature as well as on the order K up to which the asymptotic series expansions of the equations can be driven.

All solutions of the self-consistency equations that are presented in this article have been obtained by means of the principal iterative algorithm sketched in Figure 2. This procedure proved to be insensitive to the initial values and showed quite satisfying convergence properties in all regions of the parameter space explored so far.

For the sake of simplicity from now on we restrict ourselves to the case of a vanishing chemical potential, $\mu = 0$, which corresponds to half fermion filling due to particle-hole-symmetry of the Hamiltonian (1). Without loss of generality we always set $J \equiv 1$.

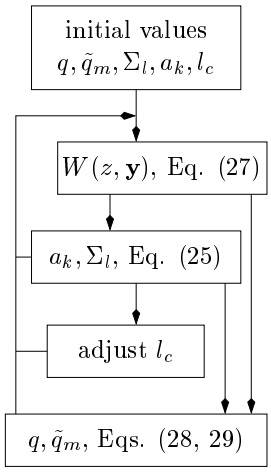

Fig. 2. Basic iterative scheme [19] for the solution of the coupled self-consistency equations (explanation in the text).

3 Spin-static approximation

This section is devoted to a discussion of the dynamical self-consistency equations in the static approximation as the first and simplest of a sequence of the dynamical approximations proposed in the last section. This static approximation consists in neglecting the time dependence of the saddle point (10) or equivalently in taking all Fourier components $\tilde{q}_m$ with $m > 0$ to be zero, *i.e.* $M = 0$. This restriction to the static component $\tilde{q}_0$ implicates tremendous simplifications of the self-consistency equations.

Because the dynamical effective fields (17) vanish the decoupling fields $y_m^{\pm}$ can be integrated out trivially. One is left with only two Gaussian integrations over the static fields y_0 and z. Also, within this approximation the occurring matrices become diagonal and thus the matrix structure of the self-consistency equations disappears. Thus, the dynamical CPA-equation (25) decouples into a set of scalar equations for each Matsubara frequency that can be solved one at a time. Furthermore, the matrix inversion (19) turns into simple scalar inversion and the evaluation of the weight function (27) reduces to an easily manageable numerical Matsubara product,

$$W_{\text{static}}(z, y_0) = \frac{1}{2}\left(\cosh\left(H_0/T\right) + 1\right) \times \prod_{l=0}^{\infty} \left(\frac{|u_l|^2 + {H_0}^2}{z_l^2 + {H_0}^2} \right)^2, \quad (32)$$

where $H_0 = \sqrt{q}\, z + \sqrt{\tilde{q}_0 - q}\, y_0$. The first term in (32) is the suitable regularized frequency and spin product of $iz_l + \sigma H_0$ and constitutes the weight function of the non-itinerant model [11]. In the present itinerant model the effect of the hopping becomes noticeable in the deviation of u_l from iz_l, where the first is defined by

$$u_l = \frac{1}{T_0(iz_l - \Sigma_l, t)} + \Sigma_l. \quad (33)$$

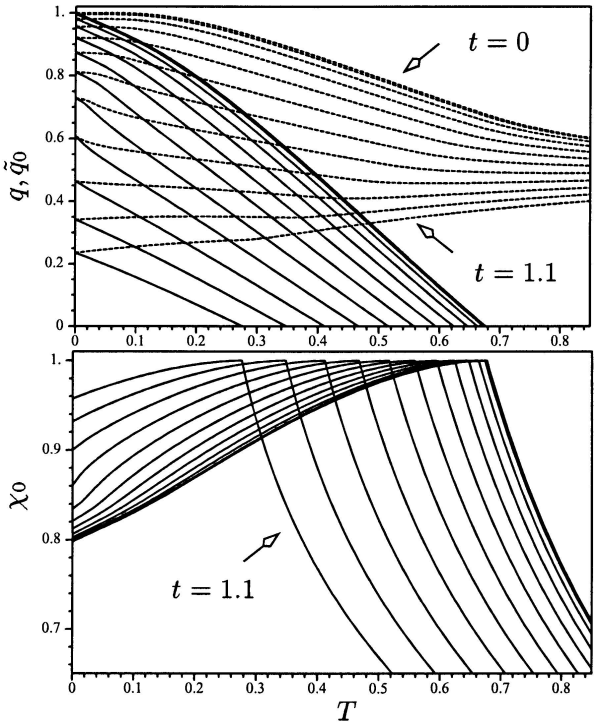

Fig. 3. Finite temperature results in the spin-static approximation for hopping strengths $t = 0 \ldots 1.1$ in steps of 0.1. The upper plot shows the spin glass order parameter q (full lines) and the zero frequency component of the replica diagonal saddle point value $\tilde{q}_0$ (dashed lines). The $\tilde{q}_0$-curves approach 1/2 as $T \to \infty$. Below is plotted the corresponding local static susceptibility $\chi_0 = (\tilde{q}_0 - q)/T$ which remains finite as $T \to 0$. At the spin glass-paramagnet transition χ_0 always reaches unity.

In terms of the functional

$$A(x) = 4x \sum_{l=0}^{\infty} \frac{1}{|u_l|^2 + x^2} \quad (34)$$

the expressions for the saddle point values q and $\tilde{q}_0$ given in equations (28, 29) simplify to

$$q = T^2 \int_z^G \left(\left[A(H_0) \right]_{y_0}^{(z)} \right)^2, \quad (35)$$

$$\tilde{q}_0 = T^2 \int_z^G \left[A(H_0)^2 + A'(H_0) \right]_{y_0}^{(z)}. \quad (36)$$

The numerical solutions of the static set of self-consistency equations are presented in Figure 3. As $T \to \infty$ all available many particle states become equally populated and $\tilde{q}_0 \to 1/2$ since two of the four local states are magnetic. In the non-itinerant limit $t = 0$ the paramagnet to spin glass transition occurs at $T_c = 1/\left(1 + \exp\left(-1/(2T_c)\right)\right) \simeq 0.6767$. The hopping hampers the local freezing of the spins and lowers the critical temperature.

3.1 The limit of zero temperature

The numerical solutions of the static equations feature the low temperature behavior $(\tilde{q}_0 - q) \sim T$. In order to perform the zero-temperature limit it is advisable to eliminate $\tilde{q}_0$ and to formulate the equations in terms of q and the static part of the local susceptibility $\chi_0 = (\tilde{q}_0 - q)/T$ which remains finite as $T \to 0$ (Fig. 4). We replace the discrete frequencies z_l by the continuous variable ζ and recall the zero-temperature limit of the Matsubara summations,

$$T \sum_{l=0}^{\infty} f(z_l) \underset{T \to 0}{\longrightarrow} \frac{1}{2\pi} \int_0^{\infty} \mathrm{d}\zeta \, f(\zeta). \tag{37}$$

By means of the rescaling of the integration variable $\sqrt{T}\, y_0 \to y_0$ the weight function (32) together with the Gaussian factor assume the form $\exp\left(-g(z, y_0)/T\right)$. The exponent function $g(z, y_0)$ can be shown to remain finite as $T \to 0$. Thus, the y_0-integration reduces to a simple saddle point integration where the z-dependent saddle point has to be determined numerically. Finally, we derive the following set of self-consistency equations at zero temperature:

$$T_0 \left(i\zeta - \Sigma(\zeta), t\right) = \frac{1}{2} \int_z^G \sum_{\sigma = \pm 1} \frac{1}{u(\zeta) + \sigma \eta(z)}, \tag{38}$$

$$q = \tilde{q}_0 = \int_z^G \bar{A}^2(\eta(z)) \tag{39}$$

$$\chi_0 = \sqrt{\frac{2}{\pi q}} + \int_z^G \frac{\bar{A}'(\eta(z))}{1 - \chi \bar{A}'(\eta(z))} \tag{40}$$

$$\eta(z) = \chi \bar{A}(\eta(z)) + \sqrt{q}|z|, \tag{41}$$

with the functional

$$\bar{A}(x) = \frac{2x}{\pi} \int_0^{\infty} \mathrm{d}\zeta \, \frac{1}{|u(\zeta)|^2 + x^2}. \tag{42}$$

In equations (38–42), $u(\zeta)$ and $\Sigma(\zeta)$ are continuous versions of the quantities Σ_l and u_l defined in Section 2.2 and equation (33). In terms of the constant

$$\gamma = \int_0^{\infty} \mathrm{d}\zeta \, \exp\left(2\zeta^2\right) \Gamma\left(\frac{1}{2}, \zeta^2\right)^2 \tag{43}$$

the static quantum critical point is located at $t_{cs} = 2\gamma/\pi \backsimeq 1.406$. Up to a slight deviation due to different model definitions this critical value quantitatively agrees with the results obtained in [3] for the case of a semi-elliptic free energy band.

In the zero-temperature disordered phase, *i.e.* for $t > t_{cs}$, the static part of the local susceptibility is given by $\chi_0(t)|_{T=0} = (\pi t - \sqrt{\pi^2 t^2 - 4\gamma^2})/(2\gamma)$. Its deviation from the corresponding quantity in the non-interacting limit, $\chi_0(t)|_{T=0, J=0} = \gamma/(\pi t)$, signalizes the vicinity of the spin glass phase.

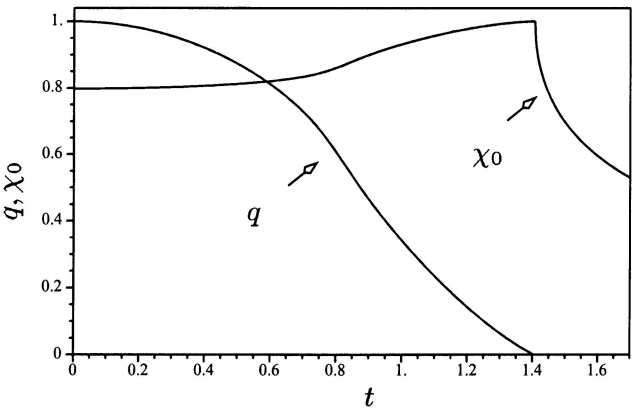

Fig. 4. Zero-temperature results for the spin glass order parameter $q = \tilde{q}_0$ and the local static susceptibility χ_0. Increasing hopping strength depresses the spin glass order and drives a zero-temperature phase transition at $t_{cs} \simeq 1.406$.

4 Quantum dynamical solutions

While exact in the non-itinerant limit, the spin-static approximation discussed in Section 3 turns out to yield a very good description of our model for weak and moderate hopping. For stronger hopping, however, this static approximation becomes increasingly inaccurate and particularly fails close to the $T = 0$ quantum phase transition. In this section we present improved solutions of the self-consistency equations within the dynamical approximation of up to third order as introduced in Section 2.3.

For the time being we restrict ourselves to the determination of the phase diagram of the model. Since at criticality there is no issue of replica symmetry breaking the choice of the replica-symmetric saddle point (10) is justified in these calculations. We determine the critical curve by virtue of the exact relation

$$T_c = \tilde{q}_0 \left(T_c\right) \tag{44}$$

which was first derived in [11] in the static approximation and can be shown to hold within the present dynamical treatment, too (see A.1). Equation (44) implies that the static part of the local susceptibility, χ_0, reaches unity at the phase transition. In solving the conditional equation (44) it is sufficient to fix the spin glass order parameter to $q = 0$ thus rendering the z-integrations in equations (25, 29) trivial.

Our solutions for the critical line $T_c(t)$ as a sequence of the first three orders of the dynamical approximation ($M = \{1, 2, 3\}$) are shown in Figure 5. With increasing hopping strength and decreasing temperature the growing influence of the discrete dynamic saddle point components $\tilde{q}_{m>0}$ is getting more and more apparent. It can be seen clearly from Figure 6 that with increasing order of the dynamical approximation two successive solutions start to separate at larger t. We observe a rapid convergence of this sequence of solutions except for the region where the quantum phase transition is expected. As $T_c \to 0$ all curves collapse into the static critical point at t_{cs}.

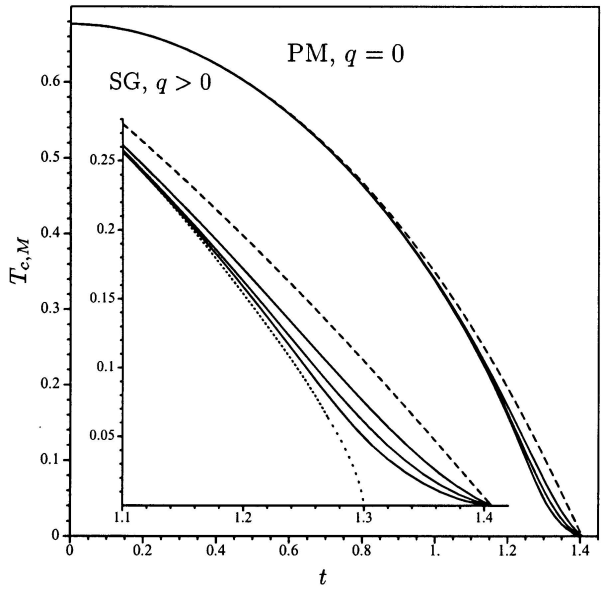

Fig. 5. The critical line of the spin glass (SG) to paramagnet (PM) phase transition in the static approximation (dashed line) and in the dynamical approximations (full lines) of first ($T_{c,1}$, uppermost) to third order as discussed in Section 2.3. The dotted line indicates the expected fully dynamical phase boundary; the light-dotted part shows the pure critical behavior (45).

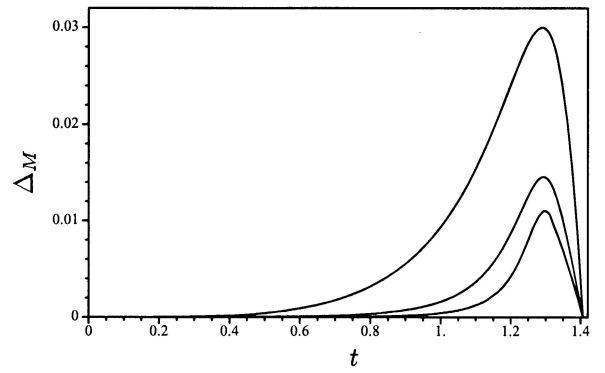

Fig. 6. Differences of the critical lines in two successive orders of the dynamical approximation, $\Delta_M = T_{c,M-1} - T_{c,M}$.

In the disordered phase the $\tilde{q}_m$ and consequently the effective potential matrix (20) vanish linearly with temperature, *i.e.* the dynamical susceptibility $\chi_m = \tilde{q}_m/T$ has a finite zero-temperature limit. Hence the self-consistent inclusion of any finite number of the $\tilde{q}_m$ can affect neither the position of the QCP nor the critical exponents. In order to capture the quantum dynamical character of the problem it is necessary to take into account the $\tilde{q}_m$ over a finite range of Matsubara frequencies ω_m around $\omega_0 = 0$. Thus, the linear temperature decrease of the $\tilde{q}_m$ is compensated by the increasing number of Fourier components within a fixed frequency range and the location of the critical point is shifted towards smaller hopping strength compared to the static approximation (Sect. A.2).

Close to zero temperature the critical line behaves like

$$T_c \sim (t_c - t)^{\phi}, \quad t < t_c \tag{45}$$

with the shift exponent changing from $\phi = 1$ in the static approximation to $\phi = 2/3$ [4] due to the quantum dynamics (Sect. A.2). Figure 5 gives an impression of how this non-analytical behavior emerges from the sequence of the (analytical) approximate solutions. The differences between two successive approximations,

$$\Delta_M = T_{c,M-1} - T_{c,M}, \tag{46}$$

exhibit pronounced maxima (Fig. 6). While the positions of these maxima vary only very little they become lower in height but sharper with increasing M.

The critical lines $T_{c,M}$ are monotonically decreasing functions of t. Hence the distance between $T_{c,M}$ and the fully dynamical true critical line, $\Delta_M^{\infty} = T_{c,M} - T_{c,\infty}$, possesses a non-analytical maximum exactly at t_c for any M. Since

$$\Delta_M^{\infty} = \sum_{M'=M+1}^{\infty} \Delta_{M'}, \tag{47}$$

this non-analyticity must coincide with the position of the maxima of the Δ_M as $M \to \infty$. This simply means that the sequence of the critical lines $T_{c,M}$ converges slowest in the very proximity of the QCP. Based on this scenario we estimate the location of the QCP: we plot the maxima positions *vs.* their heights and extrapolate to zero height. This simple procedure yields the final result

$$t_c \simeq 1.30. \tag{48}$$

5 Summary and outlook

We considered a fermionic spin glass model including a nearest-neighbor hopping term. By means of standard decoupling techniques the problem has been reduced to that of a dynamical random field system. A set of self-consistency equations for the spin glass order parameter q and the Fourier components of the replica-diagonal saddle point $\tilde{q}_m$ has been derived by virtue of a dynamical CPA method. In order to facilitate numerical solutions we kept only a manageable number of low frequency components $\tilde{q}_{m \leq M}$ in the equations and abstained from the self-consistent evaluation of the $\tilde{q}_{m>M}$. We referred to this scheme as the dynamical approximation of order M.

Within the static approximation ($\tilde{q}_{m>0} = 0$) we presented solutions both at finite and zero temperature. The second order $T = 0$ phase transition was found at $t_{cs} = 2\gamma/\pi \simeq 1.406$, equation (43). In order to determine the phase diagram of the model we calculated the SG-PM phase boundary in the dynamical approximation in up to third order (Fig. 5). These data allowed to estimate the location of the fully dynamical critical point at $t_c \simeq 1.30$. In order to confirm this result it would be desirable to find solutions in higher orders of the dynamical approximation, *i.e.* $M > 3$.

In this article we concentrated on the spin sector of our model and left out the properties in the charge sector such as the fermionic density of states. In the future it will be of high interest to investigate the effect of the hopping on the band structure of the system, particularly on the spin glass gap at zero temperature [20]. In this context an extension of the solutions to non-zero chemical potential μ [21] is desirable, too.

There are also important questions concerning the interplay between quantum dynamics and replica symmetry breaking [22], both issues being most significant at $T = 0$.

This work was supported by the Deutsche Forschungsgemeinschaft under research project Op28/5–2 and by the SFB410. One of us (M.B.) also wishes to acknowledge the scholarship granted by the University of Würzburg.

Appendix A

A.1 Derivation of equation (44)

In order to locate the spin glass phase transition we expand equation (28) in terms of q (note that q enters the equations only in the combination $\sqrt{q}z$ by equation (16)). With the abbreviation $A(z, \mathbf{y}) = \mathrm{Tr}_{l\sigma}\sigma\Gamma_\sigma(z, \mathbf{y})$ we have

$$q = T^2 \int_z^G \left([A]_{\mathbf{y}}^{(0)} + \partial_{\sqrt{q}z} [A]_{\mathbf{y}}^{(z)} \Big|_{q=0} \sqrt{q}z \right)^2 + \mathcal{O}\left(q^2\right). \tag{49}$$

Recall the definition of the average $[\,]_{\mathbf{y}}^{(z)}$, equation (26). The symmetry relations $A(0, \mathbf{y}) = -A(0, -\mathbf{y})$ and $W(0, \mathbf{y}) = W(0, -\mathbf{y})$ readily follow from equations (16, 17, 20, 24). Hence, the first term in equation (49) vanishes by the $\mathbf{y}$-integration.

For the second term in equation (49) we need to evaluate

$$\partial_{\sqrt{q}z} WA = \left(\partial_{\sqrt{q}z} W\right) A + W \partial_{\sqrt{q}z} A. \tag{50}$$

We expand the terms $\ln\left[1 + \mathsf{V}_\sigma \mathsf{T}\right]$ and $\left[\mathsf{T}^{-1} + \mathsf{V}_\sigma\right]^{-1}$ that occur in the expressions for W and A, respectively (Eqs. (27, 24)), in powers of the matrix V_σ (20). After taking the derivative these series can be re-summed easily yielding

$$\partial_{\sqrt{q}z} W = WA, \tag{51}$$

$$\partial_{\sqrt{q}z} A = -\mathrm{Tr}_{l\sigma}\Gamma_\sigma^2. \tag{52}$$

Altogether, very close to the phase transition where, $q \simeq 0$, equation (49) reads

$$1 = T^2 \int_z^G z^2 \left(\left[\left(\mathrm{Tr}_{l\sigma}\sigma\Gamma_\sigma\right)^2 - \mathrm{Tr}_{l\sigma}\Gamma_\sigma^2 \right]_{\mathbf{y}}^{(0)} \right)^2. \tag{53}$$

The remaining Gaussian z-integration evaluates to 1. By comparing to equation (29) at $T = T_c$, the right hand side of equation (53) can be identified with $\tilde{q}_0^2/T_c^2$ which finally proves relation (44).

A.2 Expansion in small $\tilde{q}_m$

In order to extract the behavior of the critical line $T_c(t)$ at the quantum phase transition we expand the self-consistency equations in powers of the effective potential matrix V_σ (20) in the disordered phase, *i.e.* for $q = 0$. The internal summations due to the occurring matrix multiplications compensate the linear temperature decrease of the Fourier components of the dynamic saddle point, $\tilde{q}_m$. An expansion up to second order yields the following self-consistency equation for the local dynamical susceptibility $\chi_m = \tilde{q}_{|m|}/T$:

$$\chi_m = C_m \left(1 + \chi_m^2\right) - (1 - C_m\chi_m)\, T \sum_{n=-\infty}^{\infty} \frac{F_{m,n}\chi_n}{1 - C_n\chi_n}. \tag{54}$$

Using the abbreviation $X_l = 1/\left(1/T_0(iz_l - \Sigma_l, t) + \Sigma_l\right)$ (see (21)) the coefficients that occur in equation (54) are defined by

$$C_m = -2T \sum_{l=-\infty}^{\infty} X_l X_{l+m}, \tag{55}$$

$$F_{m,n} = T \sum_{l=-\infty}^{\infty} X_l X_{l+m} X_{l+n} \left(2X_l + X_{l+m+n}\right), \tag{56}$$

and the self-energy is given explicitly by

$$\Sigma_l = \frac{1}{2} X_l^2 T \sum_{m=-\infty}^{\infty} \frac{\chi_m X_{l+m}}{1 - C_m\chi_m}. \tag{57}$$

By numerical evaluation of equation (54) in the zero-temperature limit we determine a critical hopping strength $t_c \simeq 1.372$ well between the static result and the expected fully dynamical value given in Section 4.

Expansion of equations (54–56) in the hopping strength around $t_c \equiv t_c(T = 0)$ and in small frequencies ω_m finally yields the condition for the critical line at small temperatures

$$t_c - t_c(T) \sim T \sum_{\omega_m=0}^{\omega_\Lambda} \sqrt{\omega_m} - T \sum_{\omega_m=0}^{\omega_\Lambda} \sqrt{\omega_m} \Bigg|_{T\to 0}$$

$$\sim T^{3/2}. \tag{58}$$

References

1. A. Georges, G. Kotliar, W. Krauth, M. Rozenberg, Rev. Mod. Phys. **68**, 13 (1996)
2. O. Parcollet, A. Georges, Phys. Rev. B **59**, 5341 (1999)
3. R. Oppermann, M. Binderberger, Ann. Physik **3**, 494 (1994)
4. S. Sachdev, N. Read, R. Oppermann, Phys. Rev. B **52**, 10286 (1995)
5. R.J. Elliot, J.A. Krumhansl, P.L. Leath, Rev. Mod. Phys. **46**, 465 (1974)
6. R. Vlaming, D. Vollhardt, Phys. Rev. B **45**, 4637 (1992)

7. V. Janiš, Phys. Rev. B **40**, 11331 (1989)
8. V. Janiš, D. Vollhardt, Phys. Rev. B **46**, 15712 (1992)
9. Y. Kakehashi, Phys. Rev. B **45**, 7196 (1992)
10. J.L. Smith, Q. Si, Phys. Rev. B **61**, 5184 (2000)
11. R. Oppermann, A. Müller-Groeling, Nucl. Phys. B **401**, 507 (1993)
12. G. Büttner, K.D. Usadel, Phys. Rev. B **42**, 6385 (1990)
13. Y.Y. Goldschmidt, P.-Y. Lai, Phys. Rev. Lett. **64**, 2467 (1990)
14. B. Rosenow, R. Oppermann, `cond-mat/9811174` (unpublished)
15. U. Wolff, Nucl. Phys. B **225**, 391 (1983)
16. E. Müller-Hartmann, Z. Phys. B **74**, 507 (1989)
17. V.N. Popov, S.A. Fedotov, Sov. Phys. JETP **67**, 535 (1988)
18. S. Kirkpatrick, D. Sherrington, Phys. Rev. B **17**, 4384 (1978)
19. The basic algorithm was implemented with the Wolfram Mathematica language while the computationally expensive matrix operations where handled by external C routines making use of the MathLink interface
20. R. Oppermann, B. Rosenow, Phys. Rev. Lett. **80**, 4767 (1998)
21. B. Rosenow, R. Oppermann, Phys. Rev. Lett. **77**, 1608 (1996)
22. R. Oppermann, B. Rosenow, Europhys. Lett. **41**, 525 (1998)